

# Inverting the Paradigm

## *From Art to Granular Science*

**BENJAMIN LEIGHTON, FRANÇOIS GUILLARD,  
KARIN EINAV PEREZ, AND ITAI EINAV**

**ABSTRACT**

The interface between art and science is an increasingly recognized source of innovation, yet explorations tend to skew toward art reaping the benefits of scientific developments. While, today, art is often freely embraced within scientific fields, it is rarely afforded the freedom to transform scientific research. The authors explore a new paradigm of “art-inspired science” by reimagining and computationally simulating an existing artwork as a dynamic body of cohesive particles. In the process, hanging forms of “granular stalactites” are identified and subsequently reproduced in an idealized simulated system. A theoretical “stickiness” model was then developed to predict their maximum height, which could have wide technological application. Artworks may therefore serve as catalysts for distinctive scientific research, allowing a mutually productive relationship between the disciplines.

The connection between art and science has been extensively analyzed [1–5], with numerous sources acknowledging that, historically, both disciplines have frequently been concerned with the same fundamental concepts [6,7]. While their approaches are vastly different, both art and science seek to interpret the world around us. This has famously been seen through shared interest in the Fibonacci sequence, with artists recognizing the Fibonacci spiral as a guide to balancing composition and scientists such as Arthur Church exploring Fibonacci geometry in the natural world [8]. As well as acknowledging this shared motivation, the literature has increasingly sought to explore the recent upsurge in cross-pollination between art and science, which has been particularly productive through the adoption of scientific concepts into artistic endeavors [9–11].

Benjamin Leighton (engineer), School of Civil Engineering, University of Sydney, NSW 2006, Australia. Email: benjaminleighton@me.com.

François Guillard (lecturer, researcher), School of Civil Engineering, University of Sydney, NSW 2006, Australia. Email: francois.guillard@sydney.edu.au. ORCID: 0000-0003-3820-2348.

Karin Einav Perez (brand designer, artist), Brown Hotels, Tel Aviv 6380115, Israel. Email: putchnik@yahoo.com.

Itai Einav (professor, research director), School of Civil Engineering, University of Sydney, NSW 2006, Australia. Email: itai.einav@sydney.edu.au. ORCID: 0000-0003-2352-1354.

See <https://direct.mit.edu/leon/issue/55/5> for supplemental files associated with this issue.

Figure 1 highlights several examples in which artists have used modern technologies and scientific understanding at varying levels of complexity to create innovative works of art. Figure 1a presents a work from Susan Aldworth’s *Brain-scapes* series, in which the artist created etchings of a patient’s brain scans to provide a unique “portrait” of the person and an exploration into the question of self. Figure 1b, a “nano sculpture” by artist Jonty Hurwitz, displays an example of an artwork relying on cutting-edge technological developments. The artist has successfully adopted an innovative lithography process whereby the photons in a high-intensity laser beam are able to polymerize a photosensitive material and create three-dimensional forms at the same scale as a human hair. Figure 1c, akin to the scientific work that is explored below in this paper, shows an artistic exploration into the dynamics of granular patterns. The figure shows a small-scale recreation of Marinus Boezem’s 1964 *Sand Fountain*. The original work, an example of land art, saw Boezem install machines in the sandy Camargue landscape of southern France to create a fountain of sand that spewed forth from a crater at varying wind speeds. Examples such as these highlight an evolution in art that has only been possible through the incorporation of modern scientific knowledge and tools, an increasingly common trend [12–14]. On the contrary, while the use of art within science has become more prevalent [15–17], it has not been adopted to the same extent [18]. To critique this bias we explore an example of art-inspired science. In doing so, we promote an inversion of the existing paradigm and support a more balanced interaction between art and science.

The catalyst for our art-science exploration began with the artwork *Like a Rock* (Fig. 2, top left), by Karin Einav Perez (2014). The work consists of a geometric web of oil marker lines set against a background of dark India ink and blank canvas. It is one piece in the larger series *Everything Connects*, which Einav Perez developed as an exploration of unconscious connection. The artist describes the works in the series (Fig. 2) as “obsessive art” that bears similarity to the meditative sketches that many people find themselves draw-

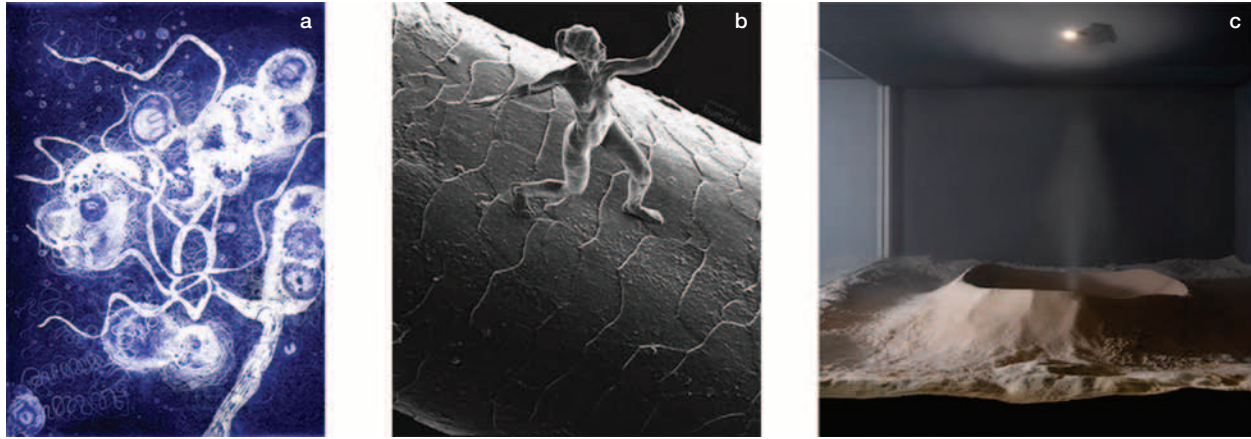


**Fig. 1.** Artists inspired by science: (a) one of Susan Aldworth's *Brainscapes*, aquatint and etching, 30 × 25 cm, 2005 (© Susan Aldworth, image courtesy of the artist); (b) Jonty Hurwitz's *Trust*, polymer nano sculpture, 80 × 100 × 20 microns, 2014 (© Jonty Hurwitz); (c) A modern, small-scale recreation (2021) of Marinus Boezem's *Sand Fountain* (1964) for the exhibition *Marinus Boezem. All Shows.* (© Marinus Boezem)

ing to keep their hands busy as they speak on the phone. Each artwork was begun with no clear final image in mind, and the artist allowed the obsessive geometric patterns to grow and take on their own forms. In doing so, Einav Perez found the shapes that naturally emerged could often be related back to memories or images that resonated with her. For example, upon reflection, the artist realized that the form seen in *Like a Rock* bore similarity to the Devils Tower rock formation featured in Steven Spielberg's *Close Encounters of the Third Kind*, one of the first films she recalls watching as a child. Despite not being grounded in any scientific theory, the artist's portrayal of geometric patterns prompted the co-authors to imagine a variety of granular phenomena. Thus, the work was seen to offer an interesting bridge between the disciplines and a launching point for art-inspired science.

From a granular physics perspective, *Like a Rock* can be imagined to reflect patterns such as sandpiles [19], angles of repose [20], and cohesive granular behavior [21–23]. The structure of the artwork itself is also reminiscent of the Delaunay contact network of a granular system [24]. With these similarities as a foundation, we started by imagining a physical, granular process from which a similar structure could emerge. In this process, a finite amount of cohesive (or “sticky”) particles are poured over an intermediate sieve and discharged through regularly spaced outlets. As they exit these outlets, some particles stick to the underside of the intermediate sieve through cohesive bonding and produce hanging formations of granular stalactites. The remainder of the particles discharge through to the floor. Eventually, clogging of the outlets allows the formation of a stable pile above.



**Fig. 2.** A selection of works from Karin Einav Perez's *Everything Connects* series, which explores the concept of “obsessive art.” The top left image, *Like a Rock* (2014), inspired the granular science of this paper. (© Karin Einav Perez)

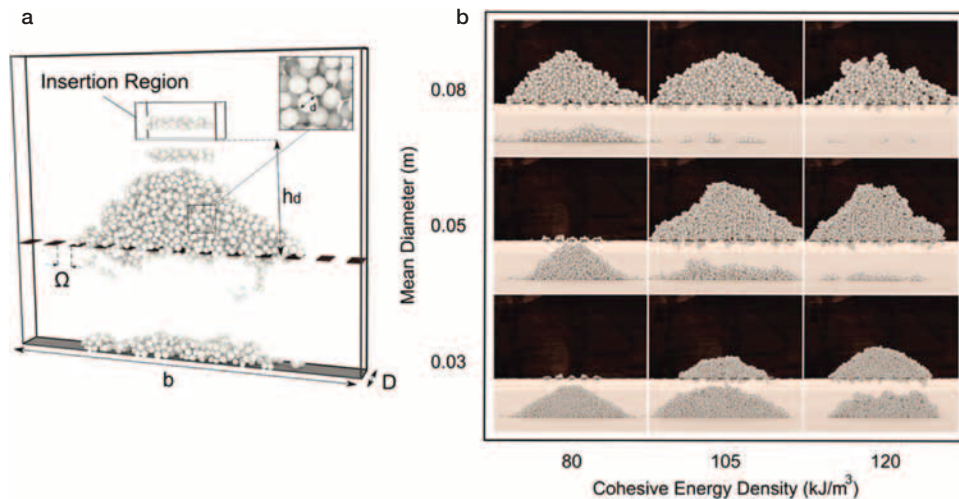


**Fig. 3.** Discrete Element Method simulations: (a) setup for the recreation of *Like a Rock*; (b) phase diagram illustrating qualitative observations of system behavior with changing diameter and cohesion.

Once at a final state of rest, a snapshot of the system's contact network would resemble the image portrayed in *Like a Rock*.

This imagined system then served as a foundation to explore a scientific process. To make the leap from art to science, we performed an investigation in two phases. Initially, we carried out a trial-and-error phase in order to recreate the artwork by simulating our imagined particulate system using a physics-based computational model of granular systems. This produced a qualitative understanding of the artwork's "scientific form" and identified the existence of cohesive hanging structures. The second phase involved additional simplified computational simulations that made it possible to quantitatively analyze these structures. While essential to the paradigm proposed, we keep the following technical description as brief as possible while leaving most of the mathematics to the Methods section in the Appendix. Those not interested in the technical process underpinning the scientific result may wish to skip to the two concluding paragraphs.

The initial qualitative understanding phase was performed by employing the Discrete Element Method (DEM) [25] to model the imagined cohesive granular system and recreate the image seen in *Like a Rock* (for further details, see Methods in the Appendix). A simulation domain (Fig. 3a) was created containing a simple mesh layer with regularly spaced, rectangular orifices. Particles of different sizes were inserted at a fixed mass rate and allowed to cascade over the mesh and filter through, until clogging occurred. For a fixed outlet width  $\Omega$ , we iteratively altered the cohesive energy density  $\kappa$  (a property that represents the ability of particles to stick), and mean particle diameter  $d$  until a system with an appearance similar to *Like a Rock* was successfully created.

It was possible to produce a number of qualitative observations about the behavior of cohesive particulate flow during this trial and error phase. In particular, we observed that the grain diameter and cohesive energy density were critical parameters in shaping the system. Figure 3b graphically summarizes the observed qualitative trends. It can be seen that both a high  $\kappa$  and large  $d$  led to early clogging that prevented sufficient material from passing through to the lower section. Conversely, small particle diameters resulted in no visible clogging and consequently prevented formation of a stable

granular pile above the mesh. This observation aligns with existing literature regarding the clogging of silos [26,27]. Low cohesion was also unsuitable due to the inability of grains to bond to the underside of the mesh.

Through a balance of these parameters, we identified a suitable range in which simulations led to a system that had high visual similarity to *Like a Rock*. Post-processing was then used to enhance the visual link, with three-dimensional high-resolution rendering performed in Blender [28] to aesthetically improve each frame individually. An animation was then created to illustrate the formation of the imagined system over time. Figures 4a–c display snapshots of this animation at various time steps. Once a steady state was reached, all particles were removed to show their centers (Fig. 4d), and the Delaunay tessellation of these particles was projected onto a 2D plane (Fig. 4e). A video of this animated process is available in supplementary materials.

During this trial-and-error recreation, we placed a large amount of focus on recreating the granular stalactites that cling from the underside of the intermediate layer. This proved the most subtle phenomenon to capture computationally but critical to understand in order to successfully recreate the artwork. Most notably, thanks to the art-driven computational exploration of these stalactites, we have identified a current gap in scientific literature surrounding the micromechanics controlling the thickness of such cohesive formations. Understanding these physics has the potential to benefit industrial granular processes where "stickiness" is a defining factor [29–31]. From our qualitative observations (Fig. 3b) it became clear that the main factors controlling these structures are grain properties.

Thus, in order to gain a more universal understanding of hanging formations beneath solid surfaces, we removed geometrical complexities and performed a second phase of simulations. In these simulations, the outlets along the horizontal plane are removed. A layer of cohesive grains of thickness  $h_0$  is first deposited against the horizontal plane (Fig. 5a). The gravity is then progressively increased from 0 to a certain  $g_c$ , at which point most of the grains detach as a block from the plane (Fig. 5b), leaving behind a limited number of grains that form hanging structures (Fig. 5c).

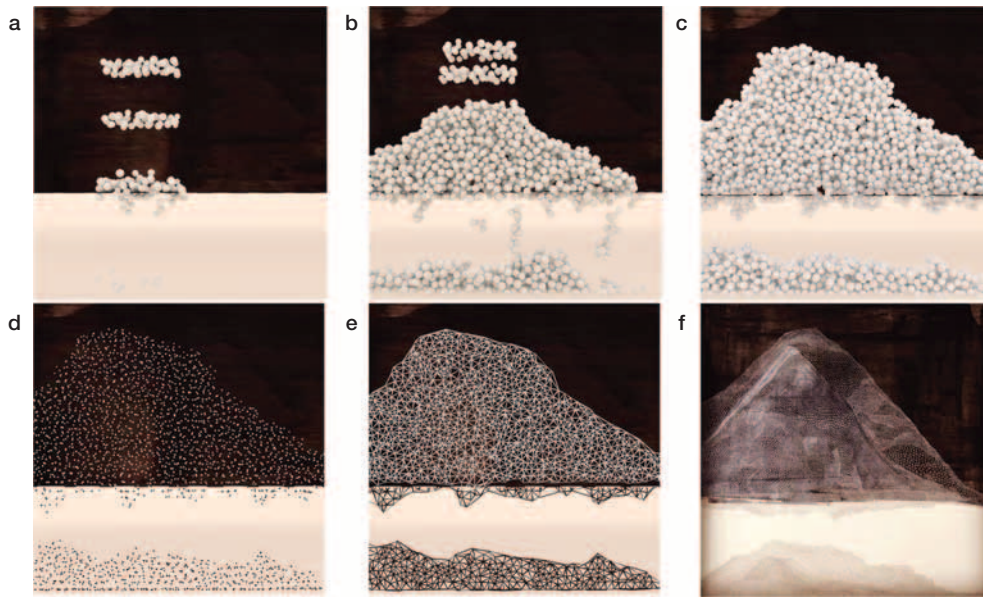


**Fig. 4.** Simulating an artwork: snapshots of the DEM simulation at (a) 0.2 seconds, (b) 2 seconds, and (c) 5 seconds; (d) particle centers projected onto a 2D plane; (e) Delaunay tessellation projected onto a 2D plane; (f) the original artwork, *Like a Rock*. For further details, see the video animation in supplementary materials.

Note that the process always involves a catastrophic detachment of a large block of grains of thickness  $h_c \sim h_0$ , as the tensile pull from the weight of the grains is maximal near the plane. As detailed in Methods in the Appendix, one can relate the maximum tension force that an individual contact could carry to the mass of the detaching layer. This defines a dimensionless proportionality coefficient  $\alpha$  (Eq. (9) in the Appendix), which is a measure of the efficiency of the random contact force network to hold the grains under gravitational pulling. Quantitatively, a regular square lattice of grains where all the contacts are the same on a given horizontal

plane would lead to detachment for  $\alpha = 1$ . However, natural grain assemblies do not follow such a regular organization. Therefore, to examine the actual value of  $\alpha$ , we assembled on Figs 5e and 5f the results of various simulations with different initial layer thicknesses and grain sizes. Figure 5e plots the measured  $\alpha$  coefficient for various grain diameters  $d$  (using two different initial layer thicknesses  $h_0$ ). Figure 5f plots the observed  $\alpha$  for various  $h_0$  (using two different  $d$ s). Note the 10 experimental points under the  $h_0 = 0.06$  m and  $d = 2$  mm cases, which were obtained using repeated experiments for different randomized initial grain locations, to examine the

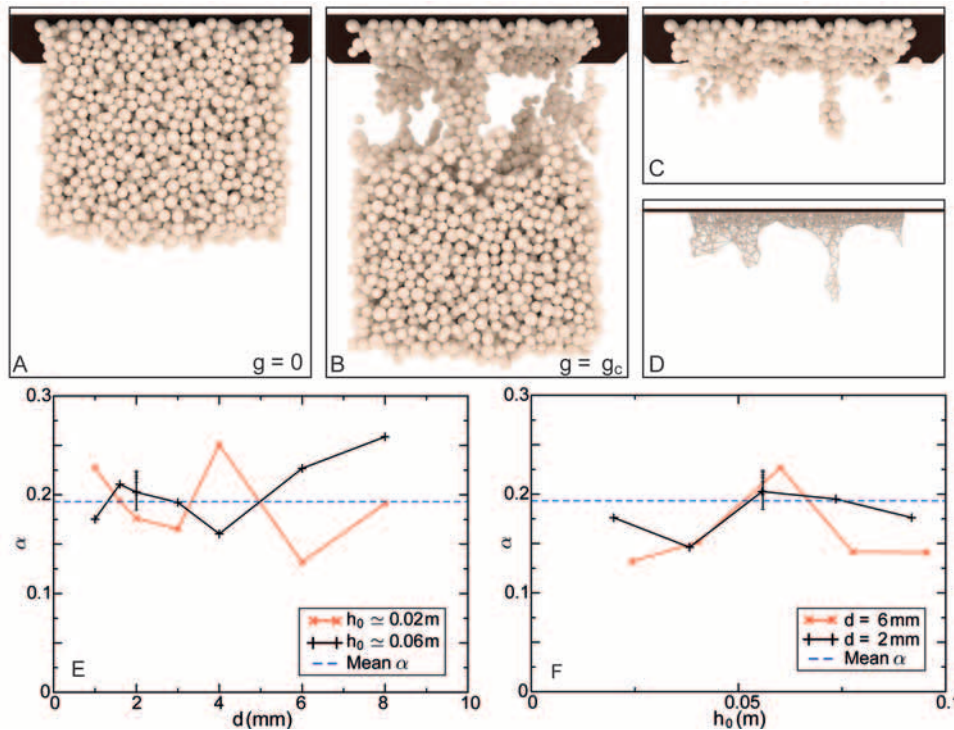


**Fig. 5.** Granular science from art: three snapshots of granular layer detachment under gravitational pulling for  $h_0 = 0.04$  m and  $d = 2$  mm. (a) initial granular layer, (b) during rupture, (c) final “stalactite” state, and (d) Delaunay tessellation of (c) using the same algorithm adopted for Fig. 4e, the measured  $\alpha$  coefficient for various grain diameters  $d$  (using two different initial layer thicknesses  $h_0$ ) and 4f for various  $h_0$  (for two different  $d$ s), respectively.

uncertainty in the  $\alpha$  measurement across the simulations. From all those simulations a representative  $\alpha \approx 0.19$  was retrieved. This low average  $\alpha$  points to the fact that the contact network is actually quite dispersed and thus ineffective at holding the suspended grain layer.

On the other hand, the absence of systematic variation of with either  $h_0$  or  $d$  shows that the physical mechanism identified to derive Eq. (9) in the Appendix is indeed at the origin of the observed dynamics. Therefore, we may rearrange that equation with the average value of  $\alpha \approx 0.19$  from the simulations to define a scaling law for the maximum thickness of granular material that could be stuck vertically under a plane for a given gravity constant  $g$ :

$$h_c = \frac{2\alpha\pi^3}{27} \frac{\kappa^3}{k_n^2 \phi \rho g}, \quad \alpha \approx 0.19, \quad (1)$$

where  $\phi \approx 0.62$  is the volume fraction of grains for dense random packings,  $\rho$  is the particle density, and  $\kappa$  and  $k_n$  are the cohesive energy and normal stiffness at contacts respectively.

Qualitatively, the finding  $\alpha < 1$  highlights the relative weakness of a dense random packing to hold itself from cohesive forces when compared with a regular square lattice of sticky grains. This could be attributed to at least three effects, namely (i) that the density of contacts on the fracture plane is not the same in random and square packings, (ii) that contact orientations are misaligned from the vertical direction and thus only partially mobilize the contact adhesion to act against the gravitational pulling force, and (iii) that only some contacts are being fully loaded due to the heterogeneity of the contact network. Considering these art-inspired realizations opens the door to future scientific research developing an analytic mathematical model that would quantitatively explain the numerically observed value of  $\alpha \approx 0.19$  for sticky granular stalactites.

This paper successfully demonstrates that consideration of artworks provokes unconventional thinking that can be adapted to produce “art-inspired science.” Through this art-inspired science, we have shown that it is possible to explore concepts that may not have been otherwise considered. If not for our curiosity regarding the artwork *Like a Rock* and subsequent desire to model a system that resembled it, it is unlikely that the authors of this paper would ever have considered hanging grain stalactites or thought to explore the mechanics of them. In developing a “stickiness model” for these stalactites, we have demonstrated that there is a tangible scientific benefit to exploring the thoughts that develop from an artistic foundation. From this one particular instance of granular stalactites, it is clear that there is potential for an inversion of the existing art-science paradigm. Just as art benefits from the technical innovations of scientific disciplines, those in the scientific community should look to draw more frequently on the creative and unorthodox thinking that is inherent to art.

Art, by its very nature, prompts each viewer to explore the artwork and find their own subjective interpretation. In fact, in discussion with a colleague, we discovered that seeing *Like a Rock* caused them immediately to think of their own

work on traffic networks. Similarly, one of the reviewers of this paper was drawn to thoughts of capillary adhesion and the Rayleigh-Plateau instability of a falling jet. While this paper has shown the success of art-inspired science specifically within the realm of granular mechanics, such alternative interpretations hint at the possibility of exploring this across a variety of disciplines. While this exploration has been seen to some extent [32,33], the attainment of a more balanced reciprocity between art and science will require it to be explored on a much larger scale.

## APPENDIX

### Methods

**DEM description.** The Discrete Element Method (DEM) simulations were performed using LIGGGHTS [34]. In the models, spherical particles interacted elastically using a Hertz contact model superposed by damping dissipation in both normal and tangential directions and cohesive force in the normal direction, while the overall tangential force was truncated by a frictional threshold. This was calculated for the normal and tangential forces, respectively, using:

$$F_n = k_n r_*^{\frac{1}{2}} \delta_n^{\frac{3}{2}} - \gamma_n (r_* \delta_n)^{\frac{1}{4}} m_*^{\frac{1}{2}} v_n - F_{\text{cohe}}, \quad (2)$$

$$F_t = \min \left[ k_t (r_* \delta_n)^{\frac{1}{2}} \delta_t - \gamma_t (r_* \delta_n)^{\frac{1}{4}} m_*^{\frac{1}{2}} v_t, \mu F_n \right], \quad (3)$$

where  $r_* = (1/r_i + 1/r_j)^{-1}$  is the weighted radius and  $m_* = (1/m_i + 1/m_j)^{-1}$  is the weighted mass of a pair of contacting  $i$  and  $j$  particles with radii  $r_i$  and  $r_j$  and masses  $m_i$  and  $m_j$ , respectively. Furthermore,  $\delta_n$  and  $\delta_t$  denote the normal and tangential interpenetrations between those particles, while  $v_n$  and  $v_t$  are their relative normal and tangential velocities. For all simulations, the following interparticle model parameters were kept constant: normal stiffness  $k_n = 3.7 \times 10^6$  Pa, tangential stiffness  $k_t = 4.5 \times 10^6$  Pa, normal damping coefficient  $\gamma_n = 2 \times 10^3$  Pa<sup>1/2</sup>, tangential damping coefficient  $\gamma_t = 1.8 \times 10^3$  Pa<sup>1/2</sup>, and friction coefficient  $\mu = 0.5$ . Particle masses were calculated given a constant particle density of  $\rho = 850$  kg. m<sup>-3</sup>. Further details on the physics behind the two laws above could be found in [35].

To model cohesive interactions between particles, the cohesive force  $F_{\text{cohe}}$  was calculated using the simple SJKR (Simple Johnson Kendall Robertson) [36] model of cohesion. This model is computationally efficient as it relates the cohesive force only to a simplified cohesive energy density and to the contact area  $A_{\text{contact}}$ :

$$F_{\text{cohe}} = \kappa A_{\text{contact}} \quad (4)$$

The equations of motion were solved for all particles by accounting for their contact forces above using a Verlet algorithm with timestep  $dt = 10^{-6}$  s. Although the simulations are performed dimensionally for easier physical interpretations, all the values can be nondimensionalized using the particle diameter  $d$  as unit length,  $\rho\pi d^3/6$  as unit mass, and  $dt$  as unit time.

Two separate geometries were established for the two different DEM calculation phases of this paper. The simulation

domains were created as 3D environments with rectangular cross sections and narrow nominal depths, to save on computation time.

**DEM model for recreating Like a Rock.** The setup used to recreate *Like a Rock* (seen in Fig. 2, top left) was a rectangular box of width  $b = 0.3$  m and depth  $D = 0.02$  m, with periodic boundaries in those two directions to prevent unwanted friction with walls and preserve the dynamics of the falling mass. Particles were randomly generated at the top using a mass rate of  $0.075 \text{ kg}\cdot\text{s}^{-1}$ , using a  $\pm 20\%$  polydispersity (variation in grain size).

Particles fell from a “drop height”  $h_d = 0.1$  m under the influence of gravity until they interacted with the intermediate mesh or particles retained by the mesh. That mesh consisted of a plane with regularly spaced orifices of width  $\Omega = 13$  mm and thickness  $0.5$  mm. The cohesive strength  $\kappa$  and particle diameter  $d = 2r$  were systematically altered. Through trial and error and the phase diagram illustrated in Fig. 3b, these were identified as the critical parameters in controlling the system to the desired form.

**DEM model of hanging cohesive layers.** A simplified setup was employed to parametrically explore the height of hanging cohesive formations, where the cohesive energy is fixed to  $\kappa = 100 \text{ kJ}\cdot\text{m}^3$ . The horizontal dimensions were made equal ( $b = D = 20d$ ), and particles with  $\pm 15\%$  polydispersity in size were poured over the entire width of the simulation domain onto a solid plane with no outlets and left to settle until a final rest state was achieved (Fig. 5a). Following this, the gravity direction was very slowly reversed and its intensity gradually increased to eventually induce a catastrophic event where a layer of particles detached and fell away from the solid plane (Fig. 5b). This process left only granular stalactites attached to the plane as shown in Fig. 5c.

**Theoretical model.** To better understand the governing mechanism behind the detachment of the cohesive granular layer under gravity, we develop a simple theoretical model for the maximum cohesive layer thickness that can support its own weight under the assumption of a square lattice of contacts, which are susceptible to break on an assumed horizontal failure plane (Fig. 6).

At equilibrium, with  $v_n = 0$ , Eq. (2) can be rewritten to obtain the attractive normal force on a single contact:

$$F_{\text{att}} = \kappa_n \frac{d}{2} \delta_n - \frac{k_n}{2} \sqrt{d} \delta_n^{\frac{3}{2}}, \quad (5)$$

The maximum of  $F_{\text{att}}$  represents the highest cohesive strength that can be achieved given the grain parameters. Equation (5) was then differentiated with respect to  $\delta_n$  and equated to zero to determine the critical delta  $\delta_c$ , representing the overlap at which the interparticle attractive force reaches its maximum:

$$\delta_c = \frac{4}{9} \left( \frac{\kappa\pi}{k} \right)^2 d, \quad (6)$$

Substituting  $\delta_c$  back into Eq. (5) gives the maximum tensile force a contact can take in terms of the known parameters:

$$F_{\text{att}}^{\text{max}} \equiv \max_{\delta} (F_{\text{att}}) = \frac{2\pi^3}{27} \frac{\kappa^3}{k_n^2} d^2, \quad (7)$$

In the simulations we observe a layer of thickness  $h_c$  detaching on an essentially horizontal plane. Dimensionally, the number of breaking contacts on that plane should scale with  $D^2/d^2$ . However, in reality the actual maximum force potentially transmitted vertically through breaking contact can only be a fraction of  $F_{\text{att}}^{\text{max}}$  due to the various contact orientations and the heterogeneity of the actual force network, which may be represented by introducing a proportionality constant  $\alpha$ . Considering force equilibrium prior to detachment for a layer of sticky grains of thickness  $h$  under gravity  $g$ , we have

$$\alpha F_{\text{att}}^{\text{max}} \frac{D^2}{d^2} = D^2 h \phi g, \quad (8)$$

where  $\phi \approx 0.62$  is the volume fraction of grains for a dense random packing. Therefore, using Eq. (7) it is possible to compute  $\alpha$  directly from the simulations for the observed grain layer thickness at the point of rupture  $h_c$  under the critical gravity  $g_c$ :

$$\alpha = \frac{27}{2\pi^3} \frac{k_n^2 \phi \rho}{\kappa^3} = g_c h_c, \quad (9)$$

This relation was used to extract numerically observed values of  $\alpha$  at critical rupture points for various simulation scenarios, as shown in Fig. 5. From that figure, we find a representative  $\alpha \approx 0.19$ , which to a leading order is insensitive to the chosen grain parameters. Therefore, this numerical proportionality constant could then be used to express the practical scaling law for critical sticky layer thickness  $h_c$  under constant gravity  $g$  as given by Eq. (1).

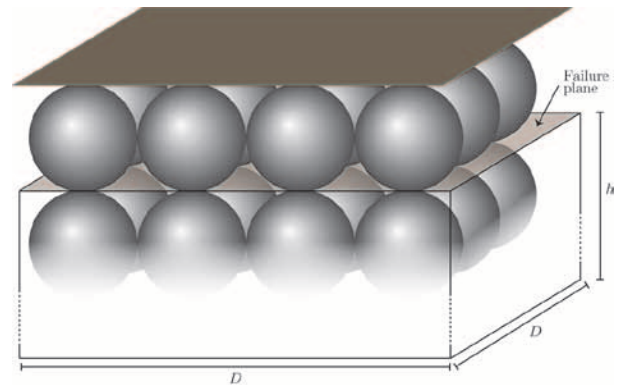


**Fig. 6.** Idealized lattice with a horizontal failure plane passing through breaking contacts at the point of rupture.

## References and Notes

- 1 R. Taylor, "From Science to Art and Back Again," *Science: Next Wave* **27** (2001).
- 2 M. Kemp, "From Science in Art to the Art of Science," *Nature* **434** (2005) pp. 308–309.
- 3 K. McMullen, "Experimental Physics, Experimental Art," *Nature* **434** (2005) pp. 310–311.
- 4 R. Lupacchini and A. Angelini, eds., *The Art of Science: From Perspective Drawing to Quantum Randomness* (Springer International Publishing, 2014).
- 5 C. Sleight and S. Craske, "Art and Science in the UK: A Brief History and Critical Reflection," *Interdisciplinary Science Reviews* **42**, No. 4, 313–330 (2017).
- 6 M. Kemp, *Structural Intuitions: Seeing Shapes in Art and Science* (Charlottesville, VA: University of Virginia Press, 2016).
- 7 N. Zabusky, "Fluids in Motion: Inspiration and Realization for Artists and STEMists," *Leonardo* **48**, No. 2, 138–146 (2015).
- 8 T. Cook, *Spirals in Nature and Art: A Study of Spiral Formations Based on the Manuscripts of Leonardo da Vinci, with Special Reference to the Architecture of the Open Staircase at Blois, in Touraine, Now for the First Time Shown to Be from His Designs* (London: J. Murray, 1903).
- 9 Kemp [2].
- 10 McMullen [3].
- 11 E. Fratreskou, "YLEM Journal: Artists Using Science Technology," *Leonardo* **42**, No. 1 (2009) p. 78.
- 12 M. Kemp, "Science in Culture," *Nature* **424** (2003) p. 18.
- 13 T. Reagan, "Ylem: Serving Artists Using Science and Technology, 1981–2009," *Leonardo* **51**, No. 1, 48–52 (2018).
- 14 I. Hediger and J. Scott, eds., *Recomposing Art and Science: Artists-in-Labs* (Berlin: De Gruyter, 2016).
- 15 E. Landhuis, "Cancer Researcher Looks to Artists for Inspiration," *Proceedings of the National Academy of Sciences* **115**, No. 5, 826–827 (2018).
- 16 R. Zattore, "Music, the Food of Neuroscience?" *Nature* **434** (2005) pp. 312–315.
- 17 J. Martin, "A Brief History of Experiments in Art and Technology," *IEEE Potentials* **34**, No. 6, 13–19 (2015).
- 18 I. Plonczak and S. Zwirn, "Understanding the Art in Science and the Science in Art Through Crosscutting Concepts," *Science Scope* **38** (2015) pp. 57–63.
- 19 H.M. Jaeger, S.R. Nagel, and R.P. Behringer, "Granular Solids, Liquids, and Gases," *Reviews of Modern Physics* **68** (1996) pp. 1259–1273.
- 20 H.M. Jaeger, C.-h. Liu, and S.R. Nagel, "Relaxation at the Angle of Repose," *Physical Review Letters* **62** (1989) p. 40.
- 21 P.G. Rognon et al., "Dense Flows of Cohesive Granular Materials," *Journal of Fluid Mechanics* **596** (2008) pp. 21–47.
- 22 P.G. Rognon et al., "Rheophysics of Cohesive Granular Materials," *Europhysics Letters* **74**, No. 4, 644–650 (2006).
- 23 S. Luding, "Cohesive, Frictional Powders: Contact Models for Tension," *Granular Matter* **10** (2008) p. 235.
- 24 B. Delaunay, "Sur la sphere vide : A la mémoire de Georges Voronoi," *Bulletin de l'Académie des Sciences de L'URSS, Classe des sciences mathématiques et naturelles* **6** (1934) pp. 793–800.
- 25 P. Cundall and O. Strack, "A Discrete Numerical Model for Granular Assemblies," *Géotechnique* **29**, No. 1, 47–65 (1979).
- 26 K. To, P. Lai, and H. Pak, "Jamming of Granular Flow in a Two-Dimensional Hopper," *Physical Review Letters* **86**, No. 1, 71–74 (2001).
- 27 K. To and P. Lai, "Jamming Pattern in a Two-Dimensional Hopper," *Physical Review E* **66** (2002).
- 28 T. Roosendaal, "Blender—A 3D Modelling and Rendering Package": [www.blender.org](http://www.blender.org).
- 29 B. Adhikari et al., "Stickiness in Foods: A Review of Mechanisms and Test Methods," *International Journal of Food Properties* **4**, No. 1, 1–33 (2001).
- 30 R. Zumsteg and A. Puzrin, "Stickiness and Adhesion of Conditioned Clay Pastes," *Tunnelling and Underground Space Technology* **31** (2012) pp. 86–96.
- 31 U. Zafar et al., "A Review of Bulk Powder Caking," *Powder Technology* **313** (2017) pp. 389–401.
- 32 R. Taylor, "Order in Pollock's Chaos," *Scientific American* **287** (2002) pp. 116–121.
- 33 E. Gates-Stuart et al., "Art and Science as Creative Catalysts," *Leonardo* **49**, No. 5, 452–453 (2016).
- 34 C. Kloss et al., "Models, Algorithms and Validation for Opensource DEM and CFD-DEM," *Progress in Computational Fluid Dynamics* **12**, Nos. 2/3, 140–152 (2012).
- 35 B. Andreotti, Y. Forterre, and O. Pouliquen, *Granular Media: Between Fluid and Solid* (Cambridge Univ. Press, 2013).
- 36 K.L. Johnson, K. Kendall, and A. Roberts, "Surface Energy and the Contact of Elastic Solids," *Proceedings of the Royal Society A* **324**, No. 1558, 301–313 (1971).

Manuscript received 27 September 2021.

**BENJAMIN LEIGHTON** is a graduate of the civil engineering faculty of the University of Sydney. He now works in the private sector and is currently engaged in the construction industry in Tokyo, Japan.

**FRANÇOIS GUILLARD** is a lecturer at the University of Sydney. His research uses numerical and experimental tools to understand granular flows and brittle porous media.

**KARIN EINAV PEREZ** is a brand designer at Brown Hotels and an established artist who is inspired both by her inner imaginative soul and by the outside world.

**ITAI EINAV** is a professor of geomechanics at the University of Sydney. His research encompasses both theoretical and applied problems related to granular and porous materials.